



Glucagon-Like Peptide-2 and the Enteric Nervous System Are Components of Cell-Cell Communication Pathway Regulating Intestinal Na⁺/Glucose Co-transport

Andrew W. Moran¹, Miran A. Al-Rammahi^{1,2}, Daniel J. Batchelor^{1†}, David M. Bravo³ and Soraya P. Shirazi-Beechey^{1*}

OPEN ACCESS

Edited by:

Catia Sternini,
University of California, Los Angeles,
United States

Reviewed by:

Sunil Yeruva,
Ludwig-Maximilians-Universität
München, Germany
Roberto De Giorgio,
University of Ferrara, Italy

*Correspondence:

Soraya P. Shirazi-Beechey
spsb@liverpool.ac.uk

†Present Address:

Daniel J. Batchelor,
Small Animal Teaching Hospital,
Institute of Veterinary Science,
University of Liverpool, Liverpool,
United Kingdom

Specialty section:

This article was submitted to
Gastrointestinal Sciences,
a section of the journal
Frontiers in Nutrition

Received: 15 May 2018

Accepted: 08 October 2018

Published: 26 October 2018

Citation:

Moran AW, Al-Rammahi MA,
Batchelor DJ, Bravo DM and
Shirazi-Beechey SP (2018)
Glucagon-Like Peptide-2 and the
Enteric Nervous System Are
Components of Cell-Cell
Communication Pathway Regulating
Intestinal Na⁺/Glucose Co-transport.
Front. Nutr. 5:101.
doi: 10.3389/fnut.2018.00101

¹ Department of Functional and Comparative Genomics, Institute of Integrative Biology, University of Liverpool, Liverpool, United Kingdom, ² Department of Medical Biotechnology, College of Biotechnology, University of Al-Qadisiyah, Al-Diwaniyah, Iraq, ³ Pancosma SA, Geneva, Switzerland

The Na⁺/glucose cotransporter 1, SGLT1 is the major route for transport of dietary glucose from the lumen of the intestine into absorptive enterocytes. Sensing of dietary sugars and artificial sweeteners by the sweet taste receptor, T1R2-T1R3, expressed in the enteroendocrine L-cell regulates SGLT1 expression in neighboring absorptive enterocytes. However, the mechanism by which sugar sensing by the enteroendocrine cell is communicated to the absorptive enterocytes is not known. Here, we show that glucagon-like peptide-2 (GLP-2) secreted from the enteroendocrine cell in response to luminal sugars regulates SGLT1 mRNA and protein expression in absorptive enterocytes, via the enteric neurons. Glucose and artificial sweeteners induced secretion of GLP-2 from mouse small intestine, which was inhibited by the sweet-taste receptor inhibitor, gurmamin. In wild type mice there was an increase in sugar-induced SGLT1 mRNA and protein abundance that was not observed in GLP-2 receptor knockout mice. GLP-2 receptor is expressed in enteric neurons, and not in absorptive enterocytes ruling out a paracrine effect of GLP-2. Electric field stimulation of the intestine resulted in upregulation of SGLT1 expression that was abolished by the nerve blocking agent tetrodotoxin. We conclude that GLP-2 and the enteric nervous system are components of the enteroendocrine-absorptive enterocyte communication pathway regulating intestinal glucose transport.

Keywords: SGLT1, regulation, glucose, intestine, GLP-2

INTRODUCTION

The Na⁺/glucose cotransporter 1, is expressed on the brush border membrane of absorptive enterocytes, and is the major route for transport of dietary glucose across the lumen of the intestine (1, 2). Absorption of glucose via SGLT1 is maximal in proximal small intestine. It has been long recognized that the activity and expression of SGLT1 is upregulated in response to increased intake of dietary carbohydrates or luminal monosaccharides (3, 4). The gut epithelium can sense luminal sugars and artificial sweetens via the G-protein coupled sweet taste receptor, T1R2-T1R3,

expressed in enteroendocrine cells to modulate its Na⁺-dependent glucose absorptive capacity (5–7). Short-term intravenous or serosal administration of GLP-2 leads to an increase in the expression of SGLT1, maximal rate of Na⁺-dependent glucose transport and an associated enhancement in blood glucose concentration (8–11). Moreover, increased levels of intracellular cAMP in absorptive enterocytes augment SGLT1 expression by enhancing the half-life of SGLT1 mRNA (12, 13), suggesting the involvement of this second messenger in the SGLT1 regulatory pathway. However, the complete endocrine cell-absorptive enterocyte communication pathway regulating intestinal Na⁺/glucose cotransport is not known.

Expression and activity of SGLT1 are significantly increased in the intestine of patients with type 2 diabetes (14) and obesity (15, 16). However, the reason for this remains unknown. Elucidating the pathway underlying regulation of SGLT1 will further our understanding of deregulation of this process in pathology. In this study our goal was to determine the mechanism by which enteroendocrine sensing of sugar regulates glucose absorptive capacity of absorptive enterocytes, and to investigate the possible role of GLP-2 in this process. Considering that the GLP-2 receptor is expressed in enteric neurons, and not in absorptive enterocytes (17, 18), we present several lines of evidence to demonstrate that GLP-2 regulates SGLT1 mRNA and protein abundance in absorptive enterocytes via a neuro-paracrine pathway. Moreover, we show that the GLP-2 dependent pathway underlying regulation of SGLT1 expression is distinct from GLP-2 induced intestinal growth.

MATERIALS AND METHODS

Reagents

All reagents were obtained from Sigma Aldrich (Poole, Dorset, UK) or Fisher Scientific (Loughborough, UK). 8-bromo-cAMP (8-Br-cAMP, B5386, Sigma) was prepared fresh immediately before use. Pituitary adenylate cyclase-activating polypeptide-38 (PACAP, A1439, Sigma), the dominant peptide in all tissues examined, was used in these experiments. Vasoactive intestinal peptide (VIP, V6130, Sigma), PACAP, corticotrophin-releasing hormone (CRH, C3042, Sigma) and calcitonin gene-related peptide (CGRP, C0168, Sigma) were dissolved in 175 mM acetic acid and substance P (S6883, Sigma) in 50 mM acetic acid with 1% (*w/v*) bovine serum albumin (A8806, Sigma). Tetrodotoxin (TTX, NA-120, Enzo Life Sciences, Exeter, UK), dissolved at 1 mg/ml in 1% (*v/v*) acetic acid, was stored at –20°C and thawed immediately before use. Peptides were stored in aliquots at –80°C and defrosted immediately before use.

Mice, Diets, and Tissue Collection

The generation of the C57BL/6 *Glp2r*^{–/–} mice has been reported previously (19). Two male and 2 female *Glp2r*^{+/-} mice were obtained from Dr. Drucker's laboratory, Toronto, Ontario. They were bred at the licensed breeding facilities at the University of Liverpool Biomedical Services Unit, to produce GLP-2 receptor knockout (*Glp2r*^{–/–}) mice and wild type offspring. Both male and female mice aged between 8 and 10 weeks were used for assessing the effect of GLP-2

receptor deletion on carbohydrate-induced regulation of SGLT1 expression. For all other experiments, male C57BL/6 mice, aged 8 week, purchased from Charles River Laboratories (Margate, Kent, UK), were utilized. All mice had access to water and food and were housed in standard tube cages with automatically controlled temperature and humidity and a 12:12 h light-dark cycle. The amount of daily food intake was similar across diets and genotype (Table S1). All mice were killed by cervical dislocation in accordance with the UK Animals (Scientific Procedures) Act, 1986 and with guidelines set out by the University of Liverpool Ethics Committee and in line with UK Home Office schedule 1 regulations. Depending on the experiment, mice were maintained either on a 40% carbohydrate (CHO)-containing diet (Testdiet #5755, energy 3.70 kcal/g, Purina Mills, Richmond, IN), or standard chow (61.8% CHO, energy 3.60 kcal/g; Special Diet Services, Witham, Essex, UK). Mice used for low/high-CHO feeding were initially kept on the 40% CHO-containing diet before switching to either a low-CHO (1.9% CHO, Testdiet #590N, energy 3.86 kcal/g,) or a high-CHO diet (69.9% CHO, Testdiet #5810, energy 3.77 kcal/g). We have previously demonstrated that SGLT1 expression is upregulated when the CHO (sucrose) content of the diet exceeds 50% (7, 20). The 5-day feeding period was selected to cover intestinal turnover from crypt to villus taking place 4–5 days (21) and 1 day dietary trial was chosen to determine if any increase occurs in existing enterocytes. All diets were isocaloric. To consider the influence of circadian periodicity on SGLT1 expression (22), mice were always killed at 10 am and diets were switched at selected times to ensure that the period of low/high CHO feeding always terminated at 10 am. Immediately after sacrifice, the entire small intestine was removed and the lumen flushed with ice cold 0.9% (*w/v*) saline and separated into three equal regions designated proximal, mid and distal. Sections of tissue (1 cm) from the proximal part of each region were fixed for immunohistochemical determinations, or frozen in liquid nitrogen for RNA analysis, with the remaining intestinal tissue being used for brush border membrane vesicle (BBMV) preparations. Tissue (1–2 cm) from C57BL/6 wild-type mice, maintained on chow, was flushed with saline, opened longitudinally and serosa removed by gentle scrapping as reported previously (23). These freshly prepared tissues were employed for gut hormone secretion assays. Hematoxylin (H) and eosin (E) staining confirmed the intactness of the villi with the serosa removed. Proximal intestine, from C57BL/6 wild-type mice maintained on the 40% CHO-containing diet, were used for electrical field stimulation studies.

Preparation of Brush-Border Membrane Vesicles

Brush border membrane vesicles (BBMV) were isolated from intestinal tissues based on the procedure described by Shirazi-Beechey et al. (24) with modifications outlined by Dyer et al. (5). All steps were carried out at 4°C. Tissues were thawed in a buffer solution [100 mM mannitol, 2 mM HEPES/Tris pH 7.1 (BP310, Fisher) with protease inhibitors, 0.5 mM dithiothreitol (D9779, Sigma), 0.2 mM benzamidine (B6506, Sigma), and 0.2 mM phenolmethylsulfonyl fluoride (P7626, Sigma)], cut into small

pieces and vibrated for 1 min at speed 5 using a FUNDAMIX vibro-mixer (Dr. Mueller AG, Maennedorf, Switzerland) in order to free epithelial cells. Subsequently, the suspension was filtered through a Büchner funnel to remove any muscle and connective tissues. The filtrate was then homogenized using a Polytron (Ystral, Reading, Berkshire, UK) for 30 s at speed 5. Next, MgCl_2 was added to the resulting homogenate to a final concentration of 10 mM and the solution stirred on ice for 20 min. The suspension was then centrifuged for 10 min at $3,000 \times g$ (SS34 rotor, Sorvell, UK) and the resulting supernatant was spun for 30 min at $30,000 \times g$. The pellet was suspended in buffer (100 mM mannitol, 0.1 mM MgSO_4 , and 20 mM HEPES/Tris pH 7.1) and homogenized with 10 strokes of a Potter Elvehjem Teflon hand-held homogenizer before centrifuging for 30 min at $30,000 \times g$. The final pellet was re-suspended in an isotonic buffer solution (buffer 3, 300 mM mannitol, 0.1 mM MgSO_4 , and 20 mM HEPES/Tris pH 7.4) and homogenized by passing through a 27-gauge needle several times. The protein concentration in the BBMV was estimated by its ability to bind Coomassie blue according to the Bio-Rad assay technique (Bio-Rad, Hemel Hempstead, UK). Porcine γ -globulin (G-2512, Sigma) was used as the standard. In preparation for western blot analysis, aliquots of freshly prepared BBMV were diluted with sample buffer [62.5 mM Tris/HCl pH 6.8, 10% (v/v) glycerol, 2% (w/v) SDS, 0.05% (v/v) β -mercaptoethanol (M-7154, Sigma), 0.05% (w/v) bromophenol blue (035730, BDH)] and stored at -20°C until use. The remaining BBMV were either diluted 1:100 in buffer 3 and stored at -20°C for enzyme activity determination or were used immediately for glucose uptake studies.

Immunohistochemistry

Mouse small intestinal tissues, removed from control and $\text{Glp2r}^{-/-}$ mice and used for single or triple immunohistochemistry were processed following protocols published previously (7, 20). Small intestinal sheets were fixed for 4 h in 4% paraformaldehyde (P/0840/53, Fisher) and then placed in 20% (w/v) sucrose (84100, Fluka, Gillingham, Dorset, UK) in PBS overnight. Subsequently, tissue samples were gelatin embedded [7.5% (w/v) gelatin G1890, Sigma, 15% (w/v) sucrose] and frozen in liquid nitrogen cooled isopentane and then kept at -80°C until use. Tissue sections (10 μm thick) were sectioned on a cryostat (Leica, CM 1900UV-1-1, Milton Keynes, Buckinghamshire, UK), thaw mounted onto polylysine coated slides and washed five times for 5 min each in PBS. Slides were then incubated for 1 h in blocking solution. For procedures using antibodies to T1R2 and T1R3 the blocking solution consisted of 5% (w/v) sucrose, 3% (w/v) bovine serum albumin (A9647, Sigma), 2% (v/v) donkey serum, and 0.1% (w/v) sodium azide in PBS, whereas the blocking solution for procedures using antibodies to VPAC1, VPAC2 (VIP/PACAP receptors 1 & 2) and GLP-2, consisted of 3% (w/v) bovine serum albumin, 2% (v/v) donkey serum, and 0.1% (w/v) sodium azide in PBS. Tissues were incubated at 4°C overnight with primary antibodies. Antibodies to T1R2 (1:750, sc-22456), T1R3 (1:750, sc-50353), GLP-2 (1:100, sc-7781), VPAC1 (1:100, sc-15958), and VPAC2 (1:100, sc-15961), were purchased from

Santa Cruz Biotechnology, INC., Santa Cruz, CA, USA. The composition of the buffer containing antibodies (primary and secondary) was 2.5% (v/v) donkey serum, 0.25% (w/v) NaN_3 and 0.2% (v/v) triton X-100 (H5141, Sigma) in PBS. For triple immunohistochemistry, two serial tissue sections were incubated with primary antibodies. One section was incubated with two primary antibodies raised in different species whilst the adjacent section was incubated with the third primary antibody. Following incubation with primary antibodies, slides were washed with PBS before incubating with secondary antibodies. Secondary antibodies were either cyanine 3-conjugated anti-goat (705-165-147) or anti-rabbit (711-165-152), raised in donkey, fluorescein isothiocyanate-conjugated anti-rabbit raised in donkey (711-095-152) purchased from Stratech Scientific Ltd (Suffolk, UK), or cyanine 3-conjugated anti-mouse raised in donkey or goat (715-165-151, Jacksons ImmunoResearch Europe Ltd., Cambridge, UK). All secondary antibodies were used at a dilution of 1:500. Finally, the slides were washed with PBS three times for 5 min and mounted in Vectashield hard set mounting media with DAPI (H-1500, Vector Laboratories, Burlington, CA, USA). The immunostaining was visualized using an epifluorescence microscope (Nikon, UK) and images were captured with a Hamamatsu digital camera (C4742-95). Images were merged using Imaging Products Laboratory software (BioVision Technologies, Exton, PA, USA).

Gut Hormone Secretion Studies

Segments of mouse intestine ($\sim 2\text{ cm}$) were prepared and treated as previously described (25). Briefly, freshly removed 2 cm segments, with the serosa removed, were incubated at 37°C , 5% CO_2 , in incubation media [500 μl , Dulbecco's modified Eagle's medium (5.55 mM glucose, D5546, Sigma) with 10% (v/v) Fetal Bovine Serum (FBS, EU-000-F, Sera Labs International, UK), 2 mM L-glutamine (G7513, Sigma), 100 U/ml penicillin/ 100 $\mu\text{g/ml}$ streptomycin (P0781, Sigma), 20 $\mu\text{l/ml}$ dipeptidyl peptidase IV inhibitor (DPP4-010, Millipore)], gassed with Carbogen (95% CO_2 , 5% O_2) and supplemented with appropriate concentrations of test agents: 10–200 mM D-glucose (10117, VWR, Leicestershire, UK), mannitol (M9647, Sigma), or artificial sweetener (10 mM, gift from Pancosma, SA, Switzerland). Control tissues were maintained simultaneously in incubation media. For treatments with gurmardin (the inhibitor of rodent T1R3) (26), tissues were first pre-incubated with 5 $\mu\text{g/ml}$ gurmardin as determined before (23, 25) for 30 min followed by incubation in media containing both gurmardin and test agents. After 1 h, incubation media were collected, centrifuged to remove cell debris, and stored at -80°C . Secretion of GLP-2 was determined using a commercial enzyme immunoassay kit (EK-028-14, Phoenix Pharmaceuticals, Phoenix Europe GmbH, Karlsruhe, Germany), following the manufacturers' instructions. The measurements were within the linear part of the standard curve.

In order to ensure that GLP-2 secretion was not biased by L-cell distribution along the length of the small intestine, parallel longitudinal gut sections for individual mice were used for each test condition. Cellular and tissue integrity were assessed histologically and by measuring the levels of lactate

dehydrogenase, a cytoplasmic marker, as described previously (23). Standard curves were constructed using GraphPad Prism 5 (GraphPad Software).

Electrical Field Stimulation (EFS)

This procedure was used as described previously (27), with modifications designed for stimulating enteric neurons. Freshly removed intact mouse proximal intestinal tissues maintained in oxygenated (Carbogen) Krebs-Henseleit buffer [110 mM NaCl (S/3160/65, Fisher), 4.7 mM KCl (P/4280/60, Fisher), 3 mM CaCl₂ (C3306, Sigma), 1.2 mM MgCl₂, 25 mM NaHCO₂ (10247, VWR), 1.15 mM NaH₂PO₄ (10245, VWR), 5.55 mM D-glucose, 4.9 mM NaPyruvate (P5280, Sigma), 2.7 mM NaFumarate (F1506, Sigma), 4.9 mM NaGlutamate (G1626, Sigma)] at 37°C were flushed with Krebs-Henseleit buffer and divided into 3 cm loops. Each loop was tied at one end with a weight attached in order for the tissue to be kept vertical. The tissue was then placed into a tissue bath containing 10 ml of Krebs-Henseleit buffer, fitted with a water jacket maintained at 37°C. Tissues were allowed to equilibrate in the bath for 20 min. Electric stimulation of the tissue was achieved using 0.5 mm diameter platinum wire electrodes, with one electrode placed inside the intestinal loop at ~3 mm to the luminal membrane and the other outside the loop at the same distance. Electrical current was applied using square wave pulses employing a Grass S44 stimulator (Natus Neurology Incorporated, Grass Products, Warwick PI, USA). The frequency was 20 Hz with duration of 0.3 ms, and delay of 1 ms using a voltage of 50 V (5 mA, measured using Keithley 6485 Instruments, Tektronix UL Ltd. Berkshire, UK). Three sets of tissue loops were used per experiment. The tissue loops which were not stimulated served as controls. One set of tissue loops that did receive EFS were preincubated with 10 μM TTX for 15 min before stimulation in TTX-containing buffer. Immediately following EFS a small section of tissue (0.5 cm) was used for mRNA isolation and the remainder of the tissue for BBMV preparation. In all three sets of tissues, control and stimulated ± TTX, immunohistochemistry showed that tissue integrity was retained and that SGLT1 expression had a similar profile; being expressed on the luminal membrane of villus enterocytes with no expression in the crypt as shown before (20, 25, 28) (data not shown).

Cell Culture

The small intestinal enterocytic cell line Caco-2/TC7 (Caco-2) cells were maintained at 37°C and 5% CO₂ in Dulbecco's modified Eagles' medium (D6546, Sigma), supplemented with 10% (v/v) fetal bovine serum, 1% (v/v) non-essential amino acid solution (M7145, Sigma), L-glutamine (2 mM), and penicillin/streptomycin (100 U/ml; 100 μg/ml) (basal medium). Six well plates were seeded with Caco-2 cells at 100,000 cells/cm² and grown to confluency (~7 d) before being incubated in media containing either 0.5 mM 8-Br-cAMP, as described before (5) or a range of concentrations of VIP, PACAP, CRH, CGRP, or Substance P. Control wells were treated with basal medium only. Equal amounts of solvents, acetic acid or acetic acid with 1% (w/v) bovine serum albumin, were included in corresponding control media. The time course of the response was determined

to establish that 24 h incubation period was the shortest period to give a reliable and significant difference in SGLT1 expression (data not shown). Cells were harvested after 24 h. Cell pellets were collected after centrifugation and frozen at -80°C until used.

Preparation of Post-nuclear Membranes

Post-nuclear membranes (PNM) were isolated as described previously (23). Caco-2 cells grown as described above (under 3.7 cell culture) were harvested and cell pellets were collected after centrifugation and frozen at -80°C until used. Caco-2 cell pellets were thawed in buffer [100 mM mannitol, 2 mM HEPES/Tris pH 7.1, 50X complete protease inhibitor cocktail (11836145001, Roche, Sigma)] and homogenized using a Polytron (10 s on setting 5) and centrifuged at 1,000 g for 10 min at 4°C, using a swing-out rotor (HB6, Sovall). The resulting supernatant was centrifuged at 30,000 g for 30 min at 4°C with the resulting pellet re-suspended in 0.5 ml buffer and transferred to a sterile Eppendorf tube and centrifuged at 30,000 g for 30 min at 4°C. The pellet was re-suspended in a buffer consisting of 300 mM mannitol, 20 mM Hepes/tris pH 7.4, 0.1 mM MgSO₄, and homogenized by passing through a 27G needle several times.

Western Blotting

BBMV were prepared as previously described (24). The abundance of SGLT1 protein in BBMV was determined by western blotting using our well characterized antibody to SGLT1 (5, 7, 20, 29). The antibody to SGLT1 was raised in rabbits (custom synthesis) to a recombinant protein corresponding to amino acids 554-640 of rabbit SGLT1, sharing 81.6% homology to the murine SGLT1 sequence. Protein components of BBMV and PNM were separated by SDS-polyacrylamide gel electrophoresis on 8% (w/v) polyacrylamide mini gels, containing 0.1% (w/v) SDS, and electrotransferred to PVDF membrane (1620264, Immun-Blot, Bio-Rad Laboratories Ltd. Hemel Hempstead, UK). Membranes were blocked by incubating for 1 h at room temperature in PBS-TM buffer (PBS containing 0.5% (w/v) non-fat dried milk (LP0031, Oxoid, UK), and 0.1% (v/v) Tween-20 (20605, Fisher) before incubation with SGLT1 antibody diluted 1:5,000 in PBS-TM. For the determination of SGLT1 protein abundance in PNM, blocking with 5% (w/v) milk and an overnight incubation at 4°C were used. Immuno-reactive bands were detected by incubation for 1 h with affinity purified horseradish peroxidase-linked anti-rabbit secondary antibody (P0217, DAKO Ltd, Cambridge, UK) diluted 1:2,000 in PBS-TM. Protein bands were visualized with WEST-one™ western blot detection system (16031, iNtRON Biotechnology, Chembio Ltd., Hertfordshire, UK) and Bio-Max Light Chemiluminescence Film (Z373508, Sigma). Scanning densitometry was performed using Total Lab (TotalLab, Newcastle-upon-Tyne, UK). Membranes were stripped by 3 × 10 min washes in 137 mM NaCl, 20 mM glycine/HCl (pH 2.5) and re-probed with a monoclonal antibody to β-actin (clone AC-15, Sigma Aldrich) used as loading controls. Blocking solution consisted of 5% (w/v) skimmed milk powder in PBS-TE (PBS, 0.1% (v/v) Triton X-100, 0.1 mM EDTA). Incubation and washing buffers were also PBS-TE. Horseradish

peroxidase-linked anti-rabbit secondary antibody (P0447, DAKO Ltd) diluted 1:2,000 in PBS-TE was used, and visualized as above.

Measurement of Na⁺-Dependent Glucose Uptake in BBMV

Na⁺-dependent glucose uptake into BBMV was measured as previously described (20, 29). The uptake of D-glucose was initiated by the addition of 100 μ l of incubation medium (100 mM NaSCN [or KSCN], 100 mM mannitol, 20 mM HEPES/Tris [pH 7.4], 0.1 mM MgSO₄, 0.02% (*w/v*) NaN₃, and 0.1 mM [U-¹⁴C]-D-glucose [10.6 GBq/mmol, NEC043X001MC, Perkin Elmer, Seer Green, Bucks, UK]) to BBMV (100 μ g protein) at 37°C. The reaction was stopped after 3 s by the addition of 1 ml of an iso-osmolar ice-cold stop buffer [150 mM KCl 20 mM HEPES/Tris (pH 7.4), 0.1 mM MgSO₄, 0.02% (*w/v*) NaN₃, and 0.1 mM phloridzin (274313, Sigma)]. Aliquots (0.9 ml) of the reaction mixture were removed and filtered under vacuum through a 0.22 μ m pore cellulose acetate/nitrate filter (GSTF02500, Millipore, Hertfordshire, UK). The filter was washed with 5 \times 1 ml of ice-cold stop buffer, placed in a vial containing 4 ml of scintillation fluid (Scintisafe 3, SC/9205/21, Fisher Scientific, UK) and the radioactivity retained on the filter was measured using a Tri-Carb 2910TR Liquid Scintillation Analyzer (PerkinElmer, Bucks, UK). All uptakes were measured in triplicate. Suitable substrate concentration, and kinetic parameters of glucose uptake were assessed previously and reported in our publications. Na⁺-dependent glucose uptake is determined by subtracting the glucose uptake in the presence of K⁺ from that of Na⁺.

Morphometry

Morphometric analysis was performed as previously described (20). Ten micrometer thick sections were exposed to tap water for 1 min, transferred to Mayer's Haemalum (3.3 mM Mayer's Haemalum-haematoxylin, 1 mM sodium iodate, 0.42 mM potassium alum; mhs16, Sigma) for 1 min and washed gently with running tap water for 5 min. They were stained with eosin Y solution [1% (*w/v*) eosin aqueous; hs250, HD Supplies, Buckingham, Bucks, UK] for 30 s and subsequently dehydrated by stepwise washing in 70% ethanol (*v/v*) for 2 \times 1-min, absolute ethanol for 2 \times 1-min, and xylene for 3 \times 1-min, before mounting with D.P.X. neutral mounting medium (317616, Sigma).

Digital images were captured with an Eclipse E400 microscope and DXM 1200 digital camera (Nikon, Kingston upon Thames, Surrey, UK), analyzed using ImageJ software (Wayne Rasband, US National Institutes of Health, Bethesda, MD) and calibrated using a 100 μ m gradient slide. The crypt depth and the villus height were measured as the average distance from crypt base to crypt-villus junction and villus base to villus tip, respectively. The villus height and the crypt depth measurements were taken from an average of 16 well oriented crypt-villus units. A minimum of three images were captured per section at a minimum of 5 sections apart. All images were captured under the same conditions with care taken to ensure that the same villus was not counted twice.

RNA Isolation and Quantitative Real-Time PCR (qPCR)

Expression of SGLT1 and VPAC1/2 mRNA was assessed by quantitative PCR as described before (23). RNA was isolated with the peqGOLD total RNA isolation kit with on-column DNase I digestion (12-6834-02, PEQLab, Hampshire, UK), and was used as template for first-strand cDNA synthesis using Superscript III reverse transcriptase (18080-044, Thermo Fisher, UK) and random hexamer primers (SO142, Fisher). cDNA was purified using QiaQuick PCR purification kit (28106, Qiagen, Crawley, UK) and qPCR assays were performed using 25 ng cDNA as template per 25 μ l reaction containing SYBR Green JumpStart Taq ReadyMix for qPCR (S4438, Sigma Aldrich) and 900 nM of each primer. PCR cycling was performed as follows: initial denaturation at 95°C for 2 min followed by 30–40 cycles of 95°C for 15 s, 60°C, for 60 s in triplicate using a Rotorgene 3000 (Qiagen, Crawley, UK). Relative abundance was calculated using RG-3000 comparative quantification software with RNA polymerase IIA (POLR2A) as control (see **Table S2** for primer sequences).

Statistics

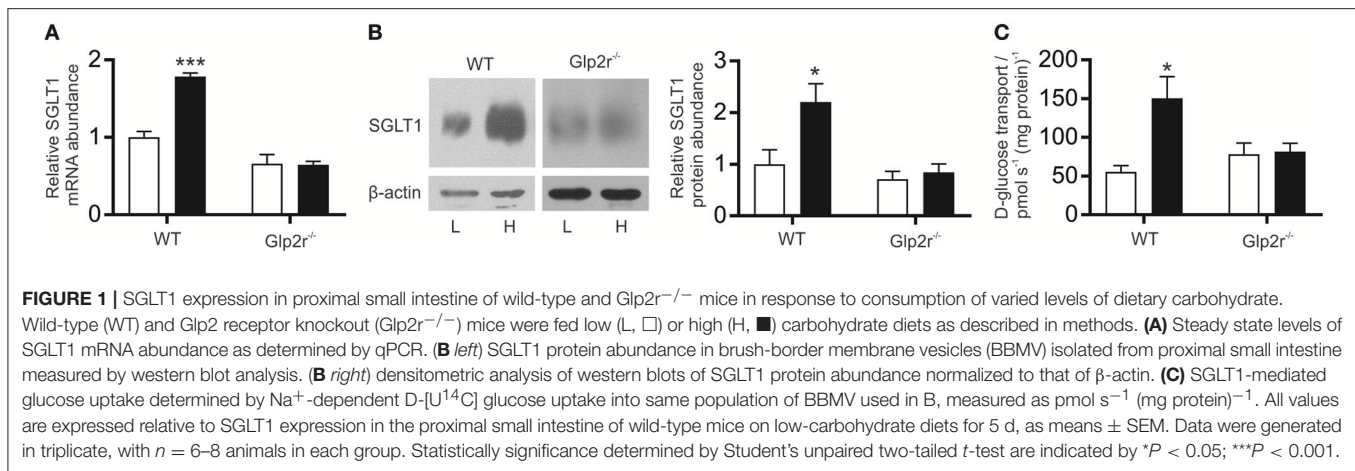
Commercial software (Graphpad Prism 5) was used for statistical analysis. D'Agostino & Pearson omnibus and Shapiro-Wilk normality tests were used to confirm that continuous variables were normally distributed. Comparison between groups was performed using Student's unpaired *t*-test and one-way ANOVA as appropriate. Dunnett's or Holm-Sidak's multiple comparison post-test was used to determine differences between groups after identification of differences by ANOVA. The level of statistical significance was set at $P < 0.05$.

RESULTS

Regulation of SGLT1 Expression in Wild-Type (WT) and GLP-2 Receptor Knockout Mice in Response to Dietary Carbohydrate

Wild type and GLP-2 receptor knockout mice were kept on diets of different carbohydrate content as we described previously (7) for 5 days before measuring intestinal expression of SGLT1. In wild type mice kept on a high- carbohydrate (70% sucrose) diet, SGLT1 mRNA abundance was 2.1-fold higher ($P < 0.0001$) than in WT mice fed a low carbohydrate (1.9% sucrose) diet (**Figure 1A**). In contrast, GLP-2 receptor knockout mice demonstrated no differences in SGLT1 mRNA expression. The amount of SGLT1 mRNA in knockout mice maintained on either diet was identical to that in wild-type mice on the low carbohydrate diet, indicating that there is a constitutive pathway, independent of GLP-2 action that maintains a basal expression level of SGLT1, and an inducible pathway dependent on GLP-2.

The abundance and activity of SGLT1 protein in brush BBMV isolated from proximal intestine were assessed by western blotting and Na⁺-dependent glucose uptake (**Figures 1B,C**). In BBMV from WT mice on the high-carbohydrate diet,



there was a 2.2-fold increase ($P = 0.300$) in SGLT1 protein abundance compared to the low-carbohydrate diet, which correlated with a 2.7-fold increase ($P = 0.0387$) in the initial rate of Na⁺-dependent glucose transport into BBMV (**Figures 1B,C**) [Rates of Na⁺-dependent glucose transport were 150.2 ± 28.2 and 55.5 ± 8.0 pmol s⁻¹ (mg protein)⁻¹ for two diet groups, respectively]; a similar increase in SGLT1 mRNA abundance and glucose transport was observed in BBMV isolated from the mid small intestine (data not shown). There was also a comparable increase in SGLT1 expression and activity when mice were maintained on low- or high-carbohydrate diets for 1 day, indicating that the increase in SGLT1 occurs in the existing enterocytes. Conversely, *GLP-2* receptor knockout mice had similar amounts of intestinal SGLT1 protein and Na⁺-dependent glucose transport when maintained on either the low- or high-carbohydrate diet. Thus, whereas wild-type mice are known to respond to increased dietary carbohydrates with enhanced SGLT1 expression (3, 7), *GLP-2* receptor knockout mice did not respond in this manner.

Immunohistochemistry showed that SGLT1 protein was expressed, irrespective of genotype, on the luminal membrane of entire villus enterocytes with no expression in the crypt; the intensity of labeling was higher in the intestine of WT mice maintained on a high carbohydrate diet (**Figure S1**).

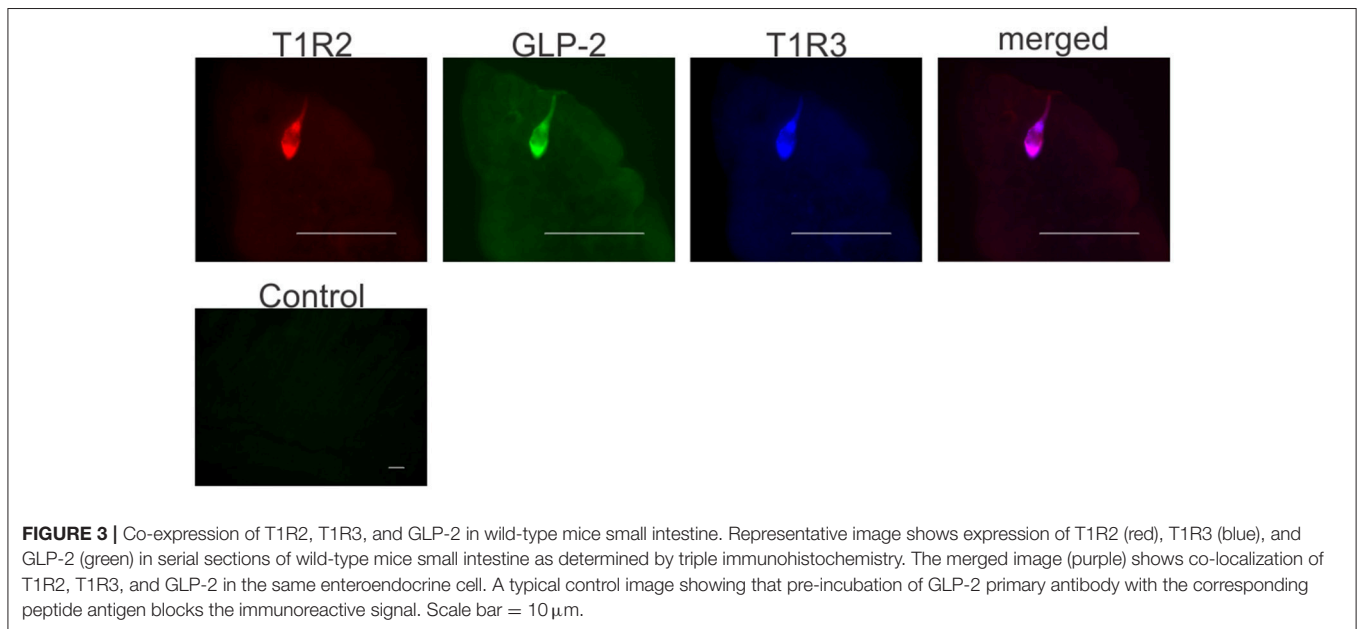
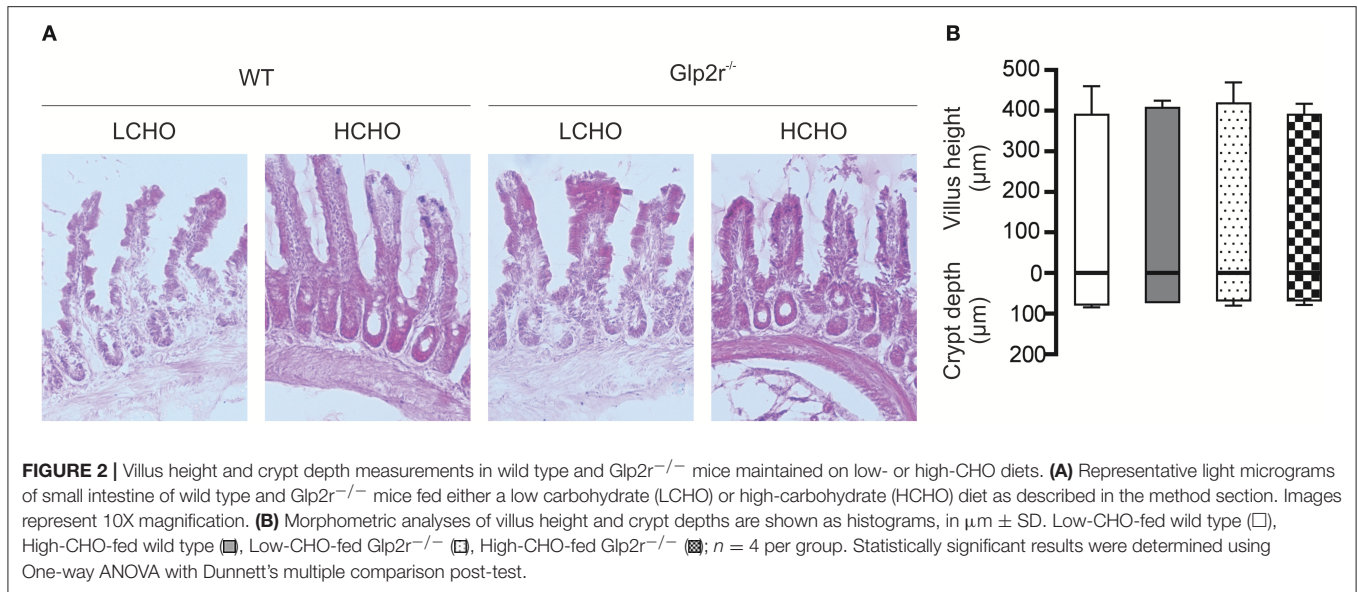
Morphometric analysis demonstrated that neither crypt-depth nor villus-height differed in the intestines of WT mice maintained on either a low- or a high-carbohydrate diet (**Figure 2**), confirming that the observed *GLP-2* induced increase in SGLT1 expression is not due to the tropic effect of *GLP-2*. Moreover, specific activity of sucrase and maltase, two brush border membrane proteins, in the intestine of WT mice maintained either on low- or high-carbohydrate diet were unchanged (**Table S3**), indicating that the *GLP-2* dependent SGLT1 regulatory pathway is distinct from the intestinotrophic effect of *GLP-2*; the latter influences villus height and the abundance of brush border membrane digestive and absorptive proteins (30).

Expression of T1R2, T1R3, and *GLP-2* in Mouse Enteroendocrine Cells

Having shown *GLP-2* involvement in the pathway regulating SGLT1 expression in response to dietary sugars, we assessed the cellular location of T1R2-T1R3 and *GLP-2* in mouse proximal intestine. Enteroendocrine cells were identified by the presence of the enteroendocrine cell marker, chromogranin A. Triple immunohistochemistry demonstrated that T1R2, T1R3, and *GLP-2* are co-expressed in the same L-enteroendocrine cell (**Figure 3**). Similar T1R2-T1R3 co-expression was observed in the intestine of the *glp2r*^{-/-} mice (**Figure S2**). Pre-incubation of *GLP-2* primary antibody with the corresponding peptide antigen blocked the immunoreactive signal, indicating specificity of labeling (**Figure 3**). T1R2 and T1R3 antibody specificity has been previously validated (7, 20, 25, 28). Approximately 30% of enteroendocrine cells contained *GLP-2*, with T1R3 and T1R2 being present in 16 and 10% of endocrine cells respectively. The cells that contained T1R2 also possessed *GLP-2* and T1R3.

Glucose and Sucralose, but Not Aspartame, Elicit *GLP-2* Release From Mouse Small Intestine

Segments of mouse proximal small intestine were incubated with increasing concentrations of D-glucose as described previously (25). Results demonstrated a dose-dependent increase in *GLP-2* secretion, with 50, 100, and 200 mM D-glucose eliciting 140 ± 14 pM (1.6-fold, $P = 0.0369$), 187 ± 13 pM (2.2-fold, $P = 0.0051$), and 245 ± 20 pM (2.8-fold $P = 0.0434$) compared to control (86.5 ± 15.5 pM), respectively (**Figure 4A**). To assess the potential effect of media osmolarity, intestinal tissues were also incubated with mannitol (10–200 mM); no *GLP-2* secretion above that of the control was observed (**Figure 4A**). When intestinal tissues were pre-incubated with gurmardin (an inhibitor of mouse T1R3) (26), glucose-induced secretion of *GLP-2* was abolished ($P = 0.0062$) (**Figure 4B**); gurmardin alone had no effect on *GLP-2* secretion. In contrast, phloridzin, an inhibitor of SGLT1 had no effect on glucose-induced *GLP-2* release



ruling out the involvement of SGLT1 as a sensor (data not shown).

To assess the effect of artificial sweeteners on GLP-2 release, mouse intestinal segments were incubated in media supplemented with either 10 mM sucralose or aspartame. Incubation with sucralose resulted in 1.5-fold ($P = 0.0026$) higher secretion of GLP-2 compared to untreated control; this was abolished when intestinal sections were pre-incubated with gurmarin ($P = 0.0088$) (**Figure 4C**). Aspartame which does not activate mouse T1R2-T1R3 (31) did not induce GLP-2 secretion (**Figure 4D**). Tissue integrity was assessed by Hematoxylin-Eosin (H&E) staining and determination of lactate dehydrogenase as reported previously (23) (**Figure S3**).

Electric Field Stimulation (EFS) of Mouse Small Intestine Enhanced SGLT1 Expression

In response to 20 min of EFS, there was a 2-fold ($P = 0.0037$) increase in SGLT1 mRNA levels (and remained the same after 30 min) compared to unstimulated tissue (**Figure 5A**). A similar increase in SGLT1 protein abundance, 2.3-fold ($P = 0.0461$), was also observed in tissues stimulated for 20 min (**Figures 5B,C**). This increase in SGLT1 expression was abolished when the tissue was pre-incubated with the neuronal sodium-channel blocker TTX (**Figures 5A-C**). TTX alone had no effect on SGLT1 expression in unstimulated tissue (data not shown).

The Effect of Modulators of Intracellular cAMP on SGLT1 Expression in Caco-2 Cells

A widely used model cell line of intestinal absorptive enterocytes, Caco-2/TC7, was used to assess expression levels of SGLT1 in

response to a number of agents known to increase intracellular cAMP. The time course of response to 8-Br-cAMP (a membrane permeable analog of cAMP) was determined in order to establish the shortest time that elicits a significant increase in SGLT1 expression. In response to 0.5 mM 8-Br-cAMP, steady-state levels of SGLT1 mRNA increased 2.3-fold ($P < 0.001$) after 24 h (Figures 5A–C).

Having shown that electric field stimulation of enteric neurons resulted in enhanced expression of SGLT1, we tested several neuropeptides for their effect on SGLT1 mRNA abundance in Caco-2 cells. The principal selection criteria were (i) established stimulatory effect on cAMP accumulation (ii) action via stimulatory GPCR (Gs), and (iii) known expression in intestinal tissue. Accordingly, VIP, PACAP, CRH, CGRP, and substance P were selected. Substance P, while acting principally via Gq, is reported to increase cAMP formation via Gs (32). Cells were exposed for 24 h to a range of concentrations (10 nM–1 μ M) of neuropeptides. In response to 100 nM VIP, there was a 1.3-fold increase in SGLT1 mRNA abundance ($P < 0.01$) with a 2-fold increase observed at 1 μ M ($P < 0.001$); the latter a similar magnitude of response to that seen after exposure to 0.5 mM 8-Br-cAMP (Figures 6A,C). The effect of PACAP also increased with concentration, with a 1.8-fold increase in SGLT1 mRNA at 100 nM and a 2.2-fold increase at 1 μ M (both $P < 0.001$; Figures 6A,D). When Caco-2 cells were incubated with 1 μ M VIP and PACAP there was a 1.7- ($P = 0.0155$) and 1.6-fold ($P = 0.0236$) increase in SGLT1 protein abundance for VIP and PACAP respectively (Figure 6B). In contrast, CRH, CGRP and Substance P had no effect on SGLT1 mRNA and protein expression (Figures 6A,B).

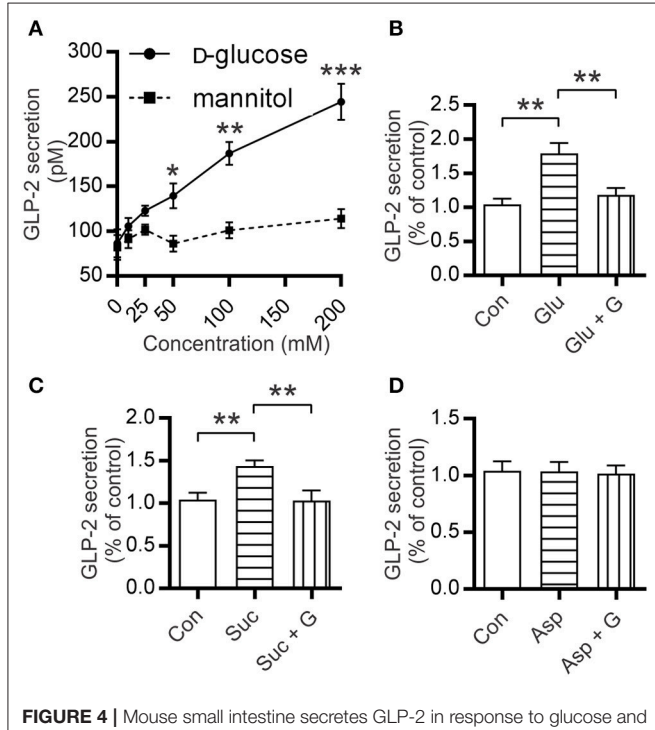


FIGURE 4 | Mouse small intestine secretes GLP-2 in response to glucose and sucralose but not aspartame. **(A)** Secretion levels of GLP-2 by mouse small intestinal tissue sections incubated at 37°C in media supplemented with increasing concentrations of glucose or mannitol. **(B–D)** Measurements of GLP-2 release in media supplemented with either 10 mM of **(B)** glucose (Glu), **(C)** sucralose (Suc), **(D)** aspartame (Asp), $\pm 5 \mu$ g/ml gurmarin (G); or untreated (Con); GLP-2 secretion was measured as described in Methods. Data are expressed as means \pm SEM. ($n = 9$ per group), where P -values are based on unpaired Student's t -tests. * $P < 0.05$, ** $P < 0.01$, and *** $P < 0.001$.

Vasoactive Intestinal Polypeptide Receptor 1 (VPAC1) Is Expressed on the Basolateral Membrane of Absorptive Enterocytes

Biological responses induced by VIP or PACAP are triggered by interaction with two receptors, VPAC1 and VPAC2, which are mainly coupled to the stimulatory G-protein, Gs, resulting

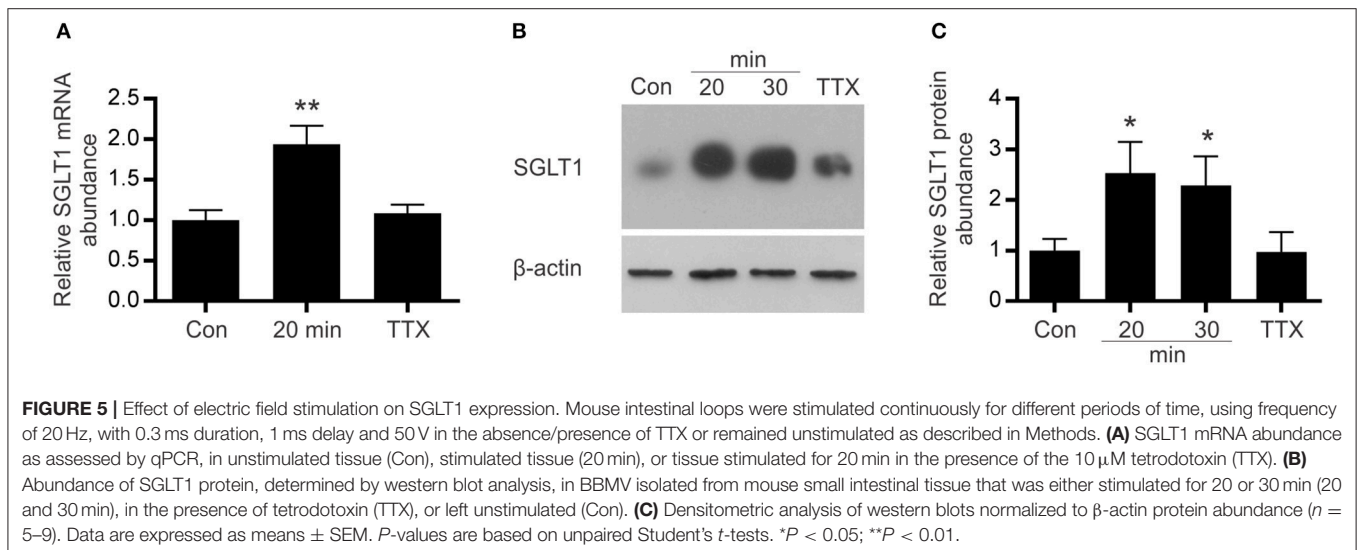
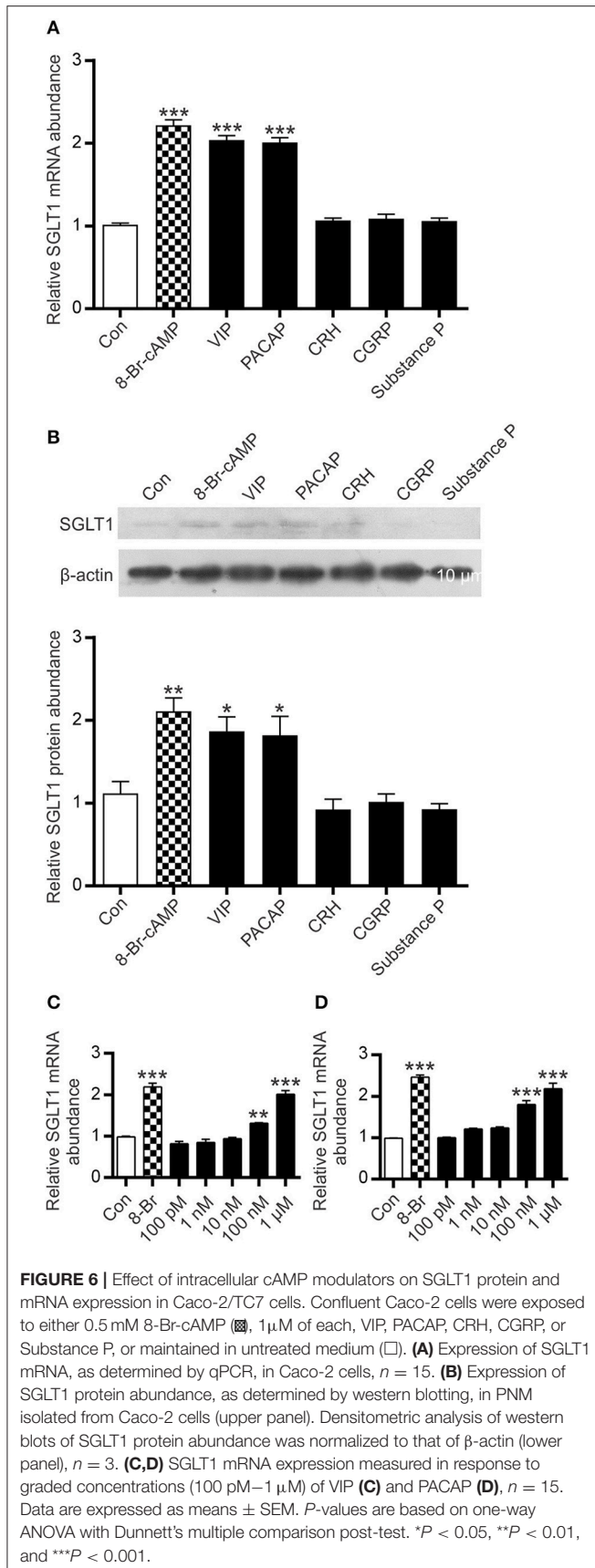


FIGURE 5 | Effect of electric field stimulation on SGLT1 expression. Mouse intestinal loops were stimulated continuously for different periods of time, using frequency of 20 Hz, with 0.3 ms duration, 1 ms delay and 50 V in the absence/presence of TTX or remained unstimulated as described in Methods. **(A)** SGLT1 mRNA abundance as assessed by qPCR, in unstimulated tissue (Con), stimulated tissue (20 min), or tissue stimulated for 20 min in the presence of the 10 μ M tetrodotoxin (TTX). **(B)** Abundance of SGLT1 protein, determined by western blot analysis, in BBMVs isolated from mouse small intestinal tissue that was either stimulated for 20 or 30 min (20 and 30 min), in the presence of tetrodotoxin (TTX), or left unstimulated (Con). **(C)** Densitometric analysis of western blots normalized to β -actin protein abundance ($n = 5$ –9). Data are expressed as means \pm SEM. P -values are based on unpaired Student's t -tests. * $P < 0.05$; ** $P < 0.01$.



in stimulation of cellular adenylate cyclase (33). Using PCR, we showed that Caco-2 cells express VPAC1 mRNA, but not VPAC2, while mouse small intestine possesses both VPAC1 and VPAC2 mRNA (data not shown). By immunohistochemistry, we demonstrated that VPAC1 is expressed on the basolateral membrane of mouse absorptive enterocytes (Figures 7A,B); whereas no labeling for VPAC2 was observed on the plasma membrane of any intestinal epithelial cells (data not shown). Pre-incubation of the antibody with the immunizing peptide blocked the labeling, showing antibody specificity (Figure 7C).

DISCUSSION

SGLT1 is expressed on the apical membrane of enterocytes, and is the major route for absorption of dietary glucose. Sensing of glucose by the sweet taste receptor, T1R2-T1R3, expressed in enteroendocrine L-cells, activates a pathway leading to upregulation of SGLT1 expression in neighboring absorptive enterocytes (7).

In response to luminal glucose, L-enteroendocrine cells secrete the gut hormone, GLP-2 (34). L-cells have been identified throughout the intestinal tract, with the highest numbers observed in the distal intestine (35). However, the proximal intestine has the greater density of GLP-2 receptor cells (36), and shows the largest response to pharmacological stimulation of the GLP-2 receptor (37, 38). GLP-2 is implicated in enhancing SGLT1 expression and intestinal glucose transport (8–11). It exerts its effect by binding to its receptor (GLP-2R).

Here, we show that knocking out the GLP-2 receptor abolishes the ability of mouse intestine to increase SGLT1 expression in response to increased dietary carbohydrate. This supports our hypothesis that GLP-2 is part of the sugar-induced pathway in the intestinal mucosa that regulates SGLT1 expression.

Immunohistochemistry on the intestinal tissues of WT and GLP2r^{-/-} mice maintained on low or high carbohydrate diets demonstrated that in all cases, irrespective of genotype and diet, SGLT1 protein is expressed on the luminal membrane of entire villus enterocytes with no labeling in the crypt. Thus, lack of response to low and high carbohydrate diet in GLP2r^{-/-} is not due to altered profile of SGLT1 protein expression along crypt-villus axis, but due to absence of receptor for GLP-2 required for this gut hormone to bind to, in order to exert its biological effect.

It is now widely recognized that GLP-2 receptor is expressed in the submucosa and myenteric plexus and not in intestinal epithelial cells (17, 18). The enteric neurons send most of their axonal projections to the muscle layers of intestine, while submucosal plexus neurons send the majority of their projections to sub-epithelial regions. The findings that GLP-2 receptor is expressed in the submucosa and myenteric plexus and not in intestinal epithelial cells rule out a direct paracrine effect of GLP-2 on neighboring absorptive enterocytes and proposes a potential role for the enteric nervous system in the regulatory pathway underlying GLP-2 induced upregulation of SGLT1 expression. Neuronal action potential mostly depends on the function of voltage gated sodium channels which are specifically inhibited by TTX (39). We show that pre-treatment of mouse intestinal

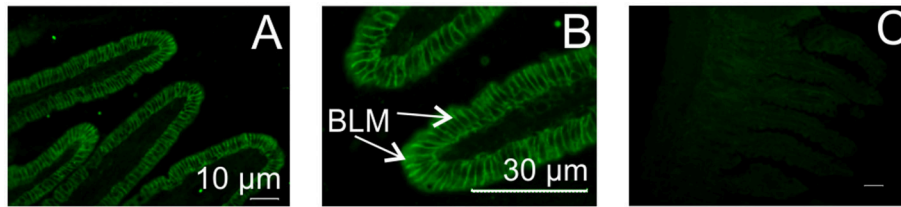


FIGURE 7 | Localization of VIP/PACAP receptor in mouse small intestine. Typical immunofluorescent images showing expression of VPAC1 protein on the basolateral membrane of mouse intestinal enterocytes (A,B). No labeling was observed with omission of the primary antibody (C, control). VPAC2 protein was not expressed. BLM, basolateral membrane.

tissue with TTX abolishes the upregulation of SGLT1 mRNA and protein in response to electric field stimulation, signifying the involvement of enteric nervous system in the regulatory process.

Increased levels of intracellular cAMP in absorptive enterocytes lead to upregulation of SGLT1 expression (12) demonstrating the involvement of this second messenger in the SGLT1 regulatory pathway. It has been shown that a number of cAMP-elevating agents increase SGLT1 expression at levels of mRNA, protein and function (5, 40) and that cAMP-induced post-transcriptional regulation of mRNA stability plays a major role in SGLT1 upregulation.

Our experimental evidence suggests that T1R2-T1R3, expressed in enteroendocrine L-cells, detects luminal glucose concentrations. When above a threshold, glucose activates a signaling pathway involving T1R2-T1R3, the associated G-protein gustducin, and other signaling elements resulting in GLP-2 secretion. The binding of GLP-2 to its receptor on the submucosal plexus elicits a neuronal response (17) which is transmitted to sub-epithelial regions through axonal projections that are in close proximity to the basolateral membrane domain of absorptive enterocytes (41) evoking the release of VIP or PACAP. Binding of VIP and/or PACAP to its receptor, VPAC1, expressed on the basolateral membrane of absorptive enterocytes, enhances intracellular levels of cAMP, thereby increasing SGLT1 expression.

It is noteworthy that VIP is released from the intestine in response to electric field stimulation (42) and that GLP-2 increases enteric neuronal expression of VIP *in vivo* (43).

It has been shown that long term GLP-2 administration results in increased crypt-villus height (44, 45) and that in the small intestine, insulin growth factor 1 (IGF-1) (and likely other growth factors such as ErbB ligands) is an essential mediator of the intestinotrophic action of GLP-2 (30, 46, 47). Assessing the intestinal tissues of WT and IGF-1 knockout mice (tissues kindly provided by Drs. Brubaker and Dubé, University of Toronto) we demonstrated that there were no differences in the expression level of SGLT1 between WT and IGF-1 knockout mice when maintained on a high (61.8%) carbohydrate diet (data not shown), indicating that the GLP-2 dependent pathway underlying regulation of SGLT1 is distinct from GLP-2 induced intestinal growth.

In the intestine of patients with type 2 diabetes, there is enhanced expression of SGLT1 mRNA, protein abundance and Na⁺-dependent D-glucose uptake (14). The increase is independent of the amount of dietary carbohydrate intake, blood glucose or insulin, and is likely to be due to deregulation of the pathway regulating expression of intestinal SGLT1 (14). The ability of the intestine to increase glucose absorption in diabetes further complicates the pathophysiology of this disease. The understanding of the regulatory pathway controlling SGLT1 expression allows identification of targets for controlling the capacity of the gut to absorb glucose. This has attendant promise for preventing and/or treating conditions such as malabsorption, diabetes and obesity.

AUTHOR CONTRIBUTIONS

SS-B is responsible for conception and design of the research with AM designing and carrying out experiments using *Glp2r*^{-/-} mice, EFS, gut hormone measurements, functional assays, western blotting and qPCR analyses of SGLT1 expression. MA-R performed all immunohistochemical analyses. SS-B and DJB designed experiments with DJB performing experiments on the effect of neuropeptides, and DMB provided nutritional advice. SS-B and AM analyzed and interpreted the data. SS-B wrote the paper.

FUNDING

AM is a postdoctoral fellow funded by Pancosma, DJB was supported by a Doctoral Training grant provided by the Biotechnology and Biological Sciences Research Council and Pfizer (UK), and MA-R by a doctoral fellowship awarded by the Iraqi Ministry of Higher Education and Scientific Research.

ACKNOWLEDGMENTS

We wish to thank Professors Daniel Drucker (Mount Sinai Hospital, Toronto) for providing *Glp2r*^{+/-} mice; David Grundy (University of Sheffield) for his advice on electric field stimulation studies, Yuzo Ninomiya (Kyushu University, Fukuoka), for the gift of gurmardin and Edith Brot-Laroche (Pierre and Marie Curie University, Paris) for provision of Caco-2/TC7 cells. We are grateful to Professor Brubaker and Dr. Dubé (University

of Toronto) for providing us with intestinal tissue from wild type mice and IGF-1 knockout mice. We wish to express our appreciation to Dr. Lynn McLaughlin of the University of Liverpool, Biomedical Services Unit for her help with breeding *Glp2r*^{-/-} mice.

REFERENCES

- Shirazi-Beechey SP. Molecular biology of intestinal glucose transport. *Nutr Res Rev.* (1995) 8:27–41. doi: 10.1079/NRR19950005
- Gorboulev V, Schürmann A, Vallon V, Kipp H, Jaschke A, Klessen D, et al. Na(+)-D-glucose cotransporter SGLT1 is pivotal for intestinal glucose absorption and glucose-dependent incretin secretion. *Diabetes* (2012) 61:87–196. doi: 10.2337/db11-1029
- Diamond JM, Karasov WH. Adaptive regulation of intestinal nutrient transporters. *Proc Natl Acad Sci USA.* (1987) 84:2242–5.
- Ferraris RP, Diamond J. Regulation of intestinal sugar transport. *Physiol Rev.* (1997) 77:257–302.
- Dyer J, Vayro S, King TP, Shirazi-Beechey SP. Glucose sensing in the intestinal epithelium. *Eur J Biochem.* (2003) 270:3377–88. doi: 10.1046/j.1432-1033.2003.03721.x
- Dyer J, Salmon KS, Zibrik L, Shirazi-Beechey SP. Expression of sweet taste receptors of the T1R family in the intestinal tract and enteroendocrine cells. *Biochem Soc Trans.* (2005) 33:302–5. doi: 10.1042/BST0330302
- Margolskee RF, Dyer J, Kokrashvili Z, Salmon KS, Ilegems E, Daly K, et al. T1R3 and gustducin in gut sense sugars to regulate expression of Na+glucose cotransporter 1. *Proc Natl Acad Sci USA.* (2007) 104:15075–80. doi: 10.1073/pnas.0706678104
- Ramsanahie A, Duxbury MS, Grikscheit TC, Perez A, Rhoads DB, Gardner-Thorpe J, et al. Effect of GLP-2 on mucosal morphology and SGLT1 expression in tissue-engineered neointestine. *Am J Physiol Gastrointest Liver Physiol.* (2003) 285:G1345–52. doi: 10.1152/ajpgi.00374.2002
- Sangild PT, Tappenden KA, Malo C, Petersen YM, Elnif J, Bartholome AL, et al. Glucagon-like peptide 2 stimulates intestinal nutrient absorption in parenterally fed newborn pigs. *J Pediatr Gastroenterol Nutr.* (2006) 43:160–67. doi: 10.1097/01.mpg.0000228122.82723.1b
- Cheeseman CI. Upregulation of SGLT-1 transport activity in rat jejunum induced by GLP-2 infusion *in vivo*. *Am J Physiol Regul Integr Comp Physiol.* (1997) 273:R1965–71.
- Burrin D, Guan X, Stoll B, Petersen YM, Sangild PT. Glucagon-like peptide 2: a key link between nutrition and intestinal adaptation in neonates? *J Nutr.* (2003) 133:3712–6. doi: 10.1093/jn/133.11.3712
- Lee WY, Loflin P, Clancey CJ, Peng H, Lever JE. Cyclic nucleotide regulation of Na+glucose cotransporter (SGLT1) mRNA stability; Interaction of a nucleocytoplasmic protein with a regulatory domain in the 3'-untranslated region critical for stabilization. *J Biol Chem.* (2000) 275:33998–4008. doi: 10.1074/jbc.M005040200
- Loflin P, Lever JE. HuR binds a cyclic nucleotide-dependent, stabilizing domain in the 3' untranslated region of Na(+)-glucose cotransporter (SGLT1) mRNA. *FEBS Lett.* (2001) 509:267–71. doi: 10.1016/S0014-5793(01)03176-3
- Dyer J, Wood IS, Palejwala A, Ellis A, Shirazi-Beechey SP. Expression of monosaccharide transporters in intestine of diabetic humans. *Am J Physiol Gastrointest Liver Physiol.* (2002) 282:G241–8. doi: 10.1152/ajpgi.00310.2001
- Nguyen NQ, Debrececi TL, Bambrick JE, Chia B, Wishart J, Deane AM, et al. Accelerated intestinal glucose absorption in morbidly obese humans: relationship to glucose transporters, incretin hormones, and glycemia. *J Clin Endocrinol Metab.* (2015) 100:968–76. doi: 10.1210/jc.2014-3144
- Wölnerhanssen BK, Moran AW, Burdya G, Meyer-Gerspach AC, Peterli R, Manz M, et al. Deregulation of transcription factors controlling intestinal epithelial cell differentiation; a predisposing factor for reduced enteroendocrine cell number in morbidly obese individuals. *Sci Rep.* (2017) 7:8174. doi: 10.1038/s41598-017-08487-9
- Bjerknes M, Cheng H. Modulation of specific intestinal epithelial progenitors by enteric neurons. *Proc Natl Acad Sci USA* (2001) 98:12497–502. doi: 10.1073/pnas.211278098
- Pedersen J, Pedersen NB, Brix SW, Grunddal KV, Rosenkilde MM, Hartmann B, et al. The glucagon-like peptide 2 receptor is expressed in enteric neurons and not in the epithelium of the intestine. *Peptides* (2015) 67:20–8. doi: 10.1016/j.peptides.2015.02.007
- Lee SJ, Lee J, Li KK, Holland D, Maughan H, Guttman DS, et al. Disruption of the murine *Glp2r* impairs Paneth cell function and increases susceptibility to small bowel enteritis. *Endocrinology* (2012) 153:1141–51. doi: 10.1210/en.2011-1954
- Moran AW, Al-Rammahi MA, Arora DK, Batchelor DJ, Coulter EA, Ionescu C, et al. Expression of Na⁺/glucose co-transporter 1 (SGLT1) in the intestine of piglets weaned to different concentrations of dietary carbohydrate. *Br J Nutr.* (2010) 104:647–55. doi: 10.1017/S0007114510000954
- Mayhew TM, Mykleburst R, Whybrow A, Jenkins R. Epithelial integrity, cell death and cell loss in mammalian small intestine. *Histol Histopathol.* (1999) 14:257–67.
- Balakrishnan A, Stearns AT, Rounds J, Irani J, Giuffrida M, Rhoads DB, et al. Diurnal rhythmicity in glucose uptake is mediated by temporal periodicity in the expression of the sodium-glucose cotransporter (SGLT1). *Surgery* (2008) 143:813–8. doi: 10.1016/j.surg.2008.03.018
- Daly K, Al-Rammahi M, Moran A, Marcello M, Ninomiya Y, Shirazi-Beechey SP. Sensing of amino acids by the gut-expressed taste receptor, T1R1-T1R3, stimulates CCK secretion. *Am J Physiol Gastrointest Liver Physiol.* (2013) 304:G271–82. doi: 10.1152/ajpgi.00074.2012
- Shirazi-Beechey SP, Davies AG, Tebbutt K, Dyer J, Ellis A, Taylor CJ, et al. Preparation and properties of brush-border membrane vesicles from human small intestine. *Gastroenterology* (1990) 98:676–85. doi: 10.1016/0016-5085(90)90288-C
- Daly K, Al-Rammahi M, Arora DK, Moran AW, Proudman CJ, Ninomiya Y, et al. Expression of sweet receptor components in equine small intestine: relevance to intestinal glucose transport. *Am J Physiol Regul Integr Comp Physiol.* (2012) 303:R199–208. doi: 10.1152/ajpregu.00031.2012
- Ninomiya Y, Imoto T. Gurmarin inhibition of sweet taste responses in mice. *Am J Physiol Regul Integr Comp Physiol.* (1995) 268:R1019–25.
- Davidson JS, Pearson GT, Petersen OH. Mouse Pancreatic Acinar Cells: Effects of electric field stimulation on membrane potential and resistance. *J Physiol.* (1980) 301:295–305.
- Batchelor DJ, Al-Rammahi M, Moran AW, Brand JG, Li X, Haskins M, et al. Intestinal sodium/glucose cotransporter-1 (SGLT1) and disaccharidase expression in the domestic dog and cat: two species of different dietary habit. *Am J Physiol Regul Integr Comp Physiol.* (2011) 300:R67–75. doi: 10.1152/ajpregu.00262.2010
- Dyer J, Hosie KB, Shirazi-Beechey SP. Nutrient regulation of human intestinal sugar transporter (SGLT1) expression. *Gut* (1997) 41:56–9.
- Rowland KJ, Brubaker PL. The “cryptic” mechanism of action of glucagon-like peptide 2. *Am J Physiol Gastrointest Liver Physiol.* (2011) 301:G1–8. doi: 10.1152/ajpgi.00039.2011
- Li X, Staszewski L, Xu H, Durick K, Zoller M, Adler E. Human receptors for sweet and umami taste. *Proc Natl Acad Sci USA.* (2002) 99:4692–6. doi: 10.1073/pnas.072090199
- Tuluc F, Lai JP, Kilpatrick LE, Evans DL, Douglas SD. Neurokinin 1 receptor isoforms and the control of innate immunity. *Trends Immunol.* (2009) 30:271–6. doi: 10.1016/j.it.2009.03.006
- Couveineau A, Ceraudo E, Tan YV, Laburthe M. VPAC1 receptor binding site: contribution of photoaffinity labeling approach. *Neuropeptides* (2010) 44:127–32. doi: 10.1016/j.npep.2009.11.008
- Drucker DJ, Yusta B. Physiology and pharmacology of the enteroendocrine hormone glucagon-like peptide-2. *Annu Rev Physiol.* (2014) 76:561–83. doi: 10.1146/annurev-physiol-021113-170317

SUPPLEMENTARY MATERIAL

The Supplementary Material for this article can be found online at: <https://www.frontiersin.org/articles/10.3389/fnut.2018.00101/full#supplementary-material>

35. Steinert RE, Gerspach AC, Gutmann H, Asarian L, Drewe J, Beglinger C. The functional involvement of gut-expressed sweet taste receptors in glucose-stimulated secretion of Glucagon-Like Peptide-1 (GLP-1) and Peptide YY (PYY). *Clin Nutr.* (2011) 30:524–32. doi: 10.1016/j.clnu.2011.01.007
36. Ørskov C, Hartmann B, Poulsen SS, Thulesen J, Hare KJ, Holst JJ. GLP-2 stimulates colonic growth via KGF, released by subepithelial myofibroblasts with GLP-2 receptors. *Regul Pept.* (2005) 124:105–12. doi: 10.1016/j.regpep.2004.07.009
37. Hare KJ, Hartmann B, Kissow H, Holst JJ, Poulsen SS. The intestinotrophic peptide, glp-2, counteracts intestinal atrophy in mice induced by the epidermal growth factor receptor inhibitor, gefitinib. *Clin Cancer Res.* (2007) 13:5170–5. doi: 10.1158/1078-0432.CCR-07-0574
38. Pedersen NB, Hjollund KR, Johnsen AH, Orskov C, Rosenkilde MM, Hartmann B, et al. Porcine glucagon-like peptide-2: structure, signaling, metabolism and effects. *Regul Pept.* (2008) 146:310–20. doi: 10.1016/j.regpep.2007.11.003
39. Bane V, Lehane M, Dikshit M, O’Riordan A, Furey A. Tetrodotoxin: chemistry, toxicity, source, distribution and detection. *Toxins* (2014) 6:693–755. doi: 10.3390/toxins6020693
40. Peng H, Lever JE. Regulation of Na(+)-coupled glucose transport in LLC-PK1 cells. Message stabilization induced by cyclic AMP elevation is accompanied by binding of a M(r) = 48,000 protein to a uridine-rich domain in the 3'-untranslated region. *J Biol Chem.* (1995) 270:23996–4003.
41. Mills JC, Gordon JI. The intestinal stem cell niche: there grows the neighborhood. *Proc Natl Acad Sci USA.* (2001) 98:12334–6. doi: 10.1073/pnas.231487198
42. Gaginella TS, O’Dorisio TM, Hubel KA. Release of vasoactive intestinal polypeptide by electrical field stimulation of rabbit ileum. *Regul Pept.* (1981) 2:165–74.
43. de Heuvel E, Wallace L, Sharkey KA, Sigalet DL. Glucagon-like peptide 2 induces vasoactive intestinal polypeptide expression in enteric neurons via phosphatidylinositol 3-kinase- γ signaling. *Am J Physiol Endocrinol Metab.* (2012) 303:E994–1005. doi: 10.1152/ajpendo.00291.2012
44. Brubaker PL, Izzo A, Hill M, Drucker DJ. Intestinal function in mice with small bowel growth induced by glucagon-like peptide-2. *Am J Physiol Endocrinol Metab.* (1997) 35:E1050–8.
45. Drucker DJ, DeForest L, Brubaker PL. Intestinal response to growth factors administered alone or in combination with human [Gly²]glucagon-like peptide 2. *Am J Physiol Gastrointest Liver Physiol.* (1997) 36:G1252–62.
46. Dubé PE, Forse CL, Bahrami J, Brubaker PL. The essential role of insulin-like growth factor-1 in the intestinal tropic effects of glucagon-like peptide-2 in mice. *Gastroenterology* (2006) 131:589–605. doi: 10.1053/j.gastro.2006.05.055
47. Leen JLS, Izzo A, Upadhyay C, Rowland KJ, Dubé PE, Gu S, et al. Mechanism of action of glucagon-like peptide-2 to increase IGF-1 mRNA in intestinal subepithelial fibroblasts. *Endocrinology* (2011) 152:436–46. doi: 10.1210/en.2010-0822

Conflict of Interest Statement: DMB was an employee of Pancosma SA.

The remaining authors declare that the research was conducted in the absence of any commercial or financial relationships that could be construed as a potential conflict of interest.

Copyright © 2018 Moran, Al-Rammahi, Batchelor, Bravo and Shirazi-Beechey. This is an open-access article distributed under the terms of the Creative Commons Attribution License (CC BY). The use, distribution or reproduction in other forums is permitted, provided the original author(s) and the copyright owner(s) are credited and that the original publication in this journal is cited, in accordance with accepted academic practice. No use, distribution or reproduction is permitted which does not comply with these terms.